DEMAZEAU, G., POUCHARD, M. & HAGENMULLER, P. (1976). *J. Solid State Chem.* **18**, 159–162.
JANSEN, M. & HOPPE, R. (1973). *Z. Anorg. Allg. Chem.* **398**, 54–62.
JANSEN, M. & HOPPE, R. (1974*a*). *Z. Anorg. Allg. Chem.* **408**, 75–82.
JANSEN, M. & HOPPE, R. (1974*b*). *Z. Anorg. Allg. Chem.* **409**, 152–162.
KISSEL, D. & HOPPE, R. (1986). *Z. Anorg. Allg. Chem.* **532**, 17–22.
KISSEL, D. & HOPPE, R. (1988). *Z. Anorg. Allg. Chem.* **559**, 40–48.
MACCHESNEY, J. B., SHERWOOD, R. C. & POTTER, J. F. (1965). *J. Chem. Phys.* **43**, 1907–1913.
MÜLLER, B. G. & HOPPE, R. (1983). *Z. Anorg. Allg. Chem.* **498**, 128–130.
O'KEEFFE, M. (1979). *Acta Cryst.* A**35**, 776–779.
O'KEEFFE, M. (1989). *Struct. Bonding (Berlin)*, **71**, 162–190.
O'KEEFFE, M. (1990). *Acta Cryst.* A**46**, 138–142.
O'KEEFFE, M. & HANSEN, S. (1988). *J. Am. Chem. Soc.* **110**, 1506–1510.
PAULING, L. (1947). *J. Am. Chem. Soc.* **69**, 542–553.
SHANNON, R. D. (1976). *Acta Cryst.* A**32**, 751–767.
STANDKE, B. & JANSEN, M. (1986). *Z. Anorg. Allg. Chem.* **535**, 39–45.
TAGUCHI, H., SHIMADA, M. & KOIZUMI, M. (1979). *J. Solid State Chem.* **29**, 221–224.
TAKEDA, Y., KANAMARU, F., SHIMADA, M. & KOIZUMI, M. (1976). *Acta Cryst.* B**32**, 2464–2466.
TAKEDA, Y., NAKA, S., TAKANO, M., SHINJO, T., TAKADA, T. & SHIMADA, M. (1978). *Mater. Res. Bull.* **13**, 61–66.
VILLARS, P. & CALVERT, L. D. (1985). *Pearson's Handbook of Crystallographic Data for Intermetallic Phases.* Metals Park, Ohio: American Society for Metals.
WELLS, A. F. (1984). *Structural Inorganic Chemistry*, 5th ed. Oxford: Clarendon Press.
WICHAINCHAI, A., DORDOR, P., DOUMERC, J. P., MARQUESTAUT, E., POUCHARD, M. & HAGENMULLER, P. (1988). *J. Solid State Chem.* **74**, 126–131.
ZACHARIASEN, W. H. (1963). *Acta Cryst.* **16**, 385–389.

Acta Cryst. (1991). B**47**, 197–206

Aluminate Sodalites: $Sr_8[Al_{12}O_{24}](MoO_4)_2$ (SAM) at 293, 423, 523, 623 and 723 K and $Sr_8[Al_{12}O_{24}](WO_4)_2$ (SAW) at 293 K

BY W. DEPMEIER

*Institut für Mineralogie und Kristallographie, TU Berlin, Sekr. BH*1, *Ernst-Reuter-Platz* 1, *D*-1000 *Berlin* 12, *Germany*

AND W. BÜHRER

Laboratorium für Neutronenstreuung, ETH Zürich, CH-5232 *Villigen PSI, Switzerland*

(*Received* 27 *June* 1990; *accepted* 9 *October* 1990)

Abstract

The crystal structure of the aluminate sodalite $Sr_8[Al_{12}O_{24}](MoO_4)_2$ (SAM) has been determined at 293 K from single-crystal X-ray data. The structure refinement was also performed employing the Rietveld method with neutron powder-diffraction data collected at nominally 293, 423, 523, 623 and 723 K. SAM is tetragonal below, but cubic above, 571 K. Crystal data: $Sr_8[Al_{12}O_{24}](MoO_4)_2$, $M_r = 1728{\cdot}6$, $F(000) = 800$; at 293 K, $I4_1/acd$, $a = 18{\cdot}8751$ (6), $c = 18{\cdot}7839$ (9) Å, $V = 6692{\cdot}1$ (7) Å^3, $Z = 8$, $D_x = 3{\cdot}43$ Mg m^{-3}; at 423 K, $I4_1/acd$, $a = 18{\cdot}9056$ (8), $c = 18{\cdot}822$ (1) Å, $V = 6727$ (1) Å^3, $Z = 8$, $D_x = 3{\cdot}41$ Mg m^{-3}; at 523 K, $I4_1/acd$, $a = 18{\cdot}9218$ (8), $c = 18{\cdot}850$ (1) Å, $V = 6749$ (1) Å^3, $Z = 8$, $D_x = 3{\cdot}40$ Mg m^{-3}; at 623 K, $Im\bar{3}m$, $a = 9{\cdot}4643$ (3) Å, $V = 847{\cdot}7$ (1) Å^3, $Z = 1$, $D_x = 3{\cdot}39$ Mg m^{-3}; at 723 K, $Im\bar{3}m$, $a = 9{\cdot}4725$ (3) Å, $V = 850{\cdot}0$ (1) Å^{-3}, $Z = 1$, $D_x = 3{\cdot}38$ Mg m^{-3}. The tetragonal phase is pyroelastic with a spontaneous-strain coefficient of about 16×10^{-4}. Structurally it is characterized by ordered arrangements of the cage anions MoO_4, which adopt the 'tetragonal orientation'. This results in conformational distortion of the sodalite framework and in displacive modulation of the Sr atoms. The cubic phase exhibits reorientational disorder of the MoO_4 tetrahedra. The temperature dependencies of lattice parameters, spontaneous-strain and atomic displacement parameters have been determined. The mean linear thermal-expansion coefficient is 12×10^{-6} K^{-1}. Structural changes, within a given phase, are smaller than the e.s.d.'s of this powder experiment. At 293 K, SAW corresponds almost perfectly to its Mo analogue: $Sr_8[Al_{12}O_{24}](WO_4)_2$, $M_r = 1904{\cdot}4$, $F(000) = 864$, $I4_1/acd$, $a = 18{\cdot}8771$ (6), $c = 18{\cdot}7819$ (9) Å, $V = 6692{\cdot}8$ (7) Å^3, $Z = 8$, $D_x = 3{\cdot}78$ Mg m^{-3}.

Introduction

SAM and SAW belong to the structural family of aluminate sodalites with general formula $M_8[Al_{12}O_{24}](XO_4)_2$, M = Ca, Sr... and X = S, Cr, Mo, W... . The structure is characterized by corner-

0108-7681/91/020197-10$03.00

sharing AlO_4 tetrahedra forming the so-called sodalite framework. The framework encloses relatively large cages, the centres of which are occupied by the tetrahedral cage anions XO_4. Adjacent sodalite cages are connected *via* common 4-rings (four AlO_4 tetrahedra) and 6-rings in the ⟨100⟩ and ⟨111⟩ directions, respectively, thus forming a body-centred cubic, space-filling arrangement. The 6-rings are the loci of the cage cations.

A major point of interest in aluminate sodalites concerns the occurrence of ferroic phase transitions, from cubic to various low-symmetry phases. For the title compounds, SAM and SAW, the transition temperatures are 571 and 609 K, respectively (Depmeier, 1988*a*). The primary driving force for these phase transitions is believed to be reorientational disorder/order processes of the cage anions. A mismatch between the relative orientations of XO_4 tetrahedra and the framework destroys the latent cubic symmetry upon ordering. The framework's and cage-cations' deviation from the cubic positions depends on a delicate balance between attractive and repulsive forces. The former act between cage cations and oxygens. The repulsive forces operate between oxygens of the cage anions and of the framework. The topological symmetry of sodalites is $Im\bar{3}m$. This reduces to $I\bar{4}3m$ if the framework undergoes 'partial collapse', *i.e.* if the volume of the unit cell shrinks as a result of cooperative rotations (tilt) of the AlO_4 tetrahedra. In the case of aluminosilicate sodalites, not considered here, Al/Si ordering may further reduce the symmetry to $P\bar{4}3n$.

According to our present knowledge, the cubic-to-noncubic phase transitions in aluminate sodalites, resulting from condensing disorder of the XO_4 tetrahedra, occur at the N point of the b.c.c. Brillouin zone. The corresponding order parameter has six components and its different physical realizations are energetically quite similar, although symmetrically different (compare, for example, Stokes & Hatch, 1988). This gives rise to a great variety of low-symmetry phases. Furthermore, as the N point belongs to the Brillouin-zone boundary, the corresponding ferroic phases are improper, and complex superstructures are normally found for the low-temperature phases.

With regard to the multicomponent order parameter, aluminate sodalites bear a certain resemblance to quite famous structural families, such as, for example, perovskites and boracites.

Virtually all aluminosilicate sodalites, and most aluminate sodalites, are partially collapsed, *i.e.* their cubic space group is $P\bar{4}3n$ or $I\bar{4}3m$, respectively. A few cases are currently known which seem to allow the centrosymmetric space group $Im\bar{3}m$, because their unit-cell volume is in accordance with a zero-tilt state of the framework. These cases are SAM, SAW and SACr, $Sr_8[Al_{12}O_{24}](CrO_4)_2$ (Depmeier, 1988*a*). In the latter case it was not possible to distinguish between $Im\bar{3}m$ and $I\bar{4}3m$ on the basis of diffraction data (Depmeier, Schmid, Setter & Werk, 1987). The phase stable below room temperature is known to be ferroelectric (Setter, Mendoza-Alvarez, Depmeier & Schmid, 1984). Thus, SACr possibly undergoes a transition from a centrosymmetric to a non-centrosymmetric state and, clearly, it was of interest to determine the corresponding symmetries and structures in the cases of SAM and SAW.

More detailed information about the aluminate sodalite family may be found in a recent review article (Depmeier, 1988*a*), and in the literature cited therein.

Experimental

The title compounds were prepared as described elsewhere (Depmeier, 1988*a*). An apparently single crystal of SAM (SAM 11/82), with good optical extinction and having the shape of a rhombic dodecahedron, dimensions approximately 0·1 × 0·1 × 0·1 mm, was chosen and mounted on a Syntex $R3$ diffractometer; graphite monochromator, Mo $K\alpha$ (λ = 0·71073 Å); 293 K; lattice parameters and orientation matrix by least squares from centring 19 strong main reflections ($8{\cdot}6 < 2\theta < 21{\cdot}3^\circ$); tetragonal spontaneous strain and intensity distribution observed; true symmetry unknown (see below); some parasitic intensity observed on plots. Owing to the lack of better single crystals, SAM 11/82 was used for the data collection, despite its obviously imperfect crystal quality; 293 K all reflections (P lattice) corresponding to an approximately 18·9 × 18·9 × 18·8 Å unit cell; $4{\cdot}5 \le 2\theta \le 60^\circ$, $0 \le h,k,l \le 27$; ω scans, scan width 0·9°, variable scan speed 2–10° min^{-1}; background measured on both sides of the reflections, total background time = 0·5 times the time used for the peaks; three standards (main reflectons), measured every 300 reflections, showed no significant change throughout the data collection; 9511 reflections; Lorentz and polarization corrections; empirical absorption correction (ψ scans), $\mu R \simeq 0{\cdot}6$, minimum/maximum transmission 0·173/0·241. Powder work performed with a double-axis multicounter powder diffractometer DMC at the Saphir reactor of the PSI [see Fischer (1985) for details of the instrument], neutrons of λ = 1·7057 Å from a Ge(311) monochromator; samples of SAM and SAW in vanadium containers of 8 mm diameter, 293 K; in a later experiment the SAM sample was measured at nominally 723, 623, 523 and 423 K. Owing to the low thermal conductivity of the sample and vanadium the temperature gradient within the sample container was high and the difference between set and real temperature was estimated to be as high as

30–40 K. The diffraction pattern was recorded between 5 and 130°, with the multicounter set at starting values 4 and 54° and two blocks of data collected at each position. The exposure time for each temperature was about 16 h and the data were corrected for absorption using the experimentally determined μR values. The background was corrected by interpolation between graphically determined points.

Structure determination

The weakness of the superstructure reflections, the marked pseudosymmetry in aluminate sodalites, and the always present possibility of pseudomerohedral/merohedral twinning (Flack, 1987) in ferroic compounds, rendered the structure determination difficult. After many trials in various tetragonal and orthorhombic space groups, with the additional assumption of several twin laws, and least-squares refinements (almost all of which gave R values well below 10% and quite 'reasonable' atomic positions for the sodalite framework and cations), the structure could be solved making use of the following observations:

(i) The fact that $|c| < |a|$ hints at 'lying' XO_4 tetrahedra (Setter & Depmeier, 1984).

(ii) The intensity distribution of the superstructure reflections, reaching quite far into the reciprocal space in the case of X-rays, indicates that the main contribution to these reflections comes from the Sr atoms.

(iii) On average, superstructure reflections with l odd are much stronger than those with l even.

Observations (ii) and (iii) are consistent with chains of Sr atoms being subject to longitudinal displacive modulation waves, running parallel to [001], and having a phase shift of π for atoms separated by $c/2$. With this assumption the intensity distribution of the superstructure reflections could be modelled and the space group determined to be either $I4_1cd$ or $I4_1/acd$.

A difference electron density map, calculated with all atoms except the MoO_4 oxygens, clearly exhibited the missing atoms and showed that the MoO_4 tetrahedra are, indeed, lying. This was taken as evidence that the space group was correct, except for the ambiguity due to the centre of symmetry.

Structure refinement

The structure refinement, with the single-crystal data of SAM, did not proceed smoothly in either space group, $I4_1/acd$ or $I4_1cd$. Restraints had to be applied to the bonds and angles within the framework in order to achieve convergence. The result was still unsatisfactory. The crystal was tested again and a considerable number of space-group forbidden reflections, with $h+k+l$ odd, were observed with intensities close to the significance threshold. Currently it is not known whether these observations correspond to inherent physical reality, *i.e.* to a symmetry of the room-temperature phase of SAM lower than $I4_1/acd$ (or $I4_1cd$), or rather to individual imperfections of the crystal used. It should be noted that the low-temperature phase of SAM is pyroelastic, if not ferroelastic, and therefore prone to the formation of stress fields around defects and domain walls. One of the reasons for deciding to switch to neutron powder diffractometry and to use Rietveld refinement (Rietveld, 1969) was to minimize these problems. The refinement in $I4_1/acd$ converged immediately. In particular, it was noted that almost all the fine details of the powder pattern, *i.e.* the superstructure reflections, were modelled very well. For the cubic phase, space group $Im\bar{3}m$ was used, rather than $I\bar{4}3m$, because of the fully-expanded framework of SAM (and SAW). The variables refined were the overall scale factor, one zero-point correction, three halfwidth parameters, lattice parameters, positional parameters (no restraints), isotropic atomic displacement parameters for sets of related atoms, *i.e.* Mo (W), XO_4 oxygens, Sr, Al and framework oxygens. The number of independent atoms was 17 in the case of $I4_1/acd$, and five for $Im\bar{3}m$. A modified version of the Wiles–Young program was used (Wiles & Young, 1981) for the Rietveld refinement. Neutron-scattering lengths (10^{-12} cm) were 0·7020 (Sr), 0·3449 (Al), 0·5803 (O), 0·6950 (Mo), 0·4770 (W). A summary of the profile refinements is given in Table 1.

Table 1. *Results of the neutron powder profile refinements*

Temp. (nominal)	Halfwidth parameter (° 2θ)^2	No. of atoms	N − P + C	R_P	R_{wp}	R_{exp}	R_B (derived)
SAM 293 K	0·73 (2) −0·75 (2) 0·27 (1)	17	1171	3·26	4·81	2·03	4·63
423 K	0·69 (2) −0·72 (3) 0·28 (1)	17	1171	4·46	5·70	2·94	8·85
523 K	0·73 (2) −0·77 (2) 0·29 (1)	17	1173	4·00	5·32	2·94	7·83
623 K	0·81 (2) −0·82 (3) 0·30 (1)	5	1258	5·14	6·66	3·01	10·08
723 K	0·75 (2) −0·79 (2) 0·29 (1)	5	1258	4·91	6·32	3·00	10·31
SAW 293 K	0·70 (2) −0·72 (2) 0·27 (1)	17	1171	3·47	4·93	2·32	4·80

Results and discussion

Tables 2(*a*) and 2(*d*) list the refined atomic positional parameters for the tetragonal (293 K) and cubic

(623 K) experimental sets of SAM. Tables 3(*a*) and 3(*d*) show, correspondingly, important interatomic distances and angles. The 423 and 523 K results of SAM and the 293 K results of SAW do not differ significantly from those of SAM at 293 K. Likewise, the results at 723 K for SAM do not differ significantly from those at 623 K. The corresponding Tables 2(*b*), 2(*c*), 2(*e*), 2(*f*), 3(*b*), 3(*c*), 3(*e*) and 3(*f*) have been deposited,* as well as plots of the observed calculated powder profiles (Figs. 1*a*–1*f*). Table 4 shows, for all experiments, important temperature-dependent quantities, such as lattice parameters, spontaneous-strain and atomic displacement parameters.

The tetragonal phase

One of the main results of the present study is the determination of the low-temperature phases of SAM and SAW. Only SAM will be discussed explicitly, because the two compounds are virtually identical. As the refinement proceeded very well in space group $I4_1/acd$, this will be regarded as the symmetry of the tetragonal phase, at least as long as no clear need for a symmetry reduction becomes evident. Even then, the present choice of space group would be a very good approximation. SAM exhibits all the structural characteristics of an ordered aluminate sodalite. The relevant details which distinguish individual species concern the question of how the different constituents, *i.e.* cage anions, cage cations and framework, are arranged with respect to one another and how they interact. The MoO_4 (WO_4) tetrahedra have the 'tetragonal orientation' (Depmeier, 1984*a*), *i.e.* they are rotated by approximately 45° about one of their local $\bar{4}$ axes, out of the hypothetical 'cubic' position, where its threefold axes would match those of the sodalite framework. There is one symmetrically independent MoO_4 (WO_4) tetrahedron per unit cell, but the symmetry operations generate a total of four essentially different orientations with respect to the unit-cell edges (see Fig. 2). Each tetrahedron has one edge parallel to *c* (V edge) and one edge parallel to either *a* or *b* (H edge). The XO_4 oxygens O(1) and O(2) form the V and H edges, respectively. The geometry of the tetrahedra does not deviate significantly from ideal values. The estimated standard deviations are, however, quite high and depend on temperature (0·1–0·4 Å for *X*—O bond lengths, 1–2° for the angles).

Table 2. *Refined atomic positional parameters* ($\times 10^3$ *at* 293 K, $\times 10^4$ *at nominally* 623 K) *for* $Sr_8[Al_{12}O_{24}](MoO_4)_2$, *SAM*

E.s.d.'s are given in parentheses.

(*a*) 293 K; space group is $I4_1/acd$ with origin choice 2

	Wyckoff notation	Site symmetry	*x*	*y*	*z*
Al(1)	32(*g*)	1	623 (1)	498 (2)	0 (1)
Al(2)	32(*g*)	1	495 (1)	624 (1)	−5 (2)
Al(3)	16(*f*)	2	246 (2)	496 (2)	125
Al(4)	8(*b*)	222	0	250	125
Al(5)	8(*a*)	$\bar{4}$	0	250	375
O(11)	32(*g*)	1	589 (1)	415 (1)	5 (1)
O(12)	32(*g*)	1	572 (1)	574 (1)	−4 (1)
O(13)	32(*g*)	1	661 (1)	497 (1)	88 (1)
O(14)	32(*g*)	1	498 (1)	669 (1)	80 (1)
O(15)	32(*g*)	1	498 (1)	330 (1)	80 (1)
O(16)	32(*g*)	1	318 (1)	498 (1)	69 (1)
Sr(1)	16(*f*)	2	122 (1)	372 (1)	125
Sr(2)	16(*f*)	2	372 (1)	622 (1)	125
Sr(3)	32(*g*)	1	377 (1)	380 (1)	119 (1)
Mo	16(*e*)	2	250	248 (2)	0
O(1)	32(*g*)	1	251 (1)	195 (1)	76 (1)
O(2)	32(*g*)	1	326 (1)	304 (1)	−2 (1)

(*d*) 623 K; space group is $Im\bar{3}m$, O_F and O_T denote framework and cage-anion O atoms, respectively

	Wyckoff notation	Site symmetry	Occupancy	*x*	*y*	*z*
Al	12(*d*)	$\bar{4}2m$	1·0	2500	5000	0
O_F	24(*h*)	*mm*	1·0	1586 (2)	1586 (2)	5000
Sr	8(*c*)	$\bar{3}m$	1·0	2500	2500	2500
Mo	2(*a*)	$m\bar{3}m$	1·0	0	0	0
O_T	24(*h*)	*mm*	¼	1277 (9)	1277 (9)	0

Fig. 2 demonstrates the arrangement of the MoO_4 tetrahedra with respect to each other and to the Sr cage cations. The Sr atoms are close to their ideal cubic positions, *i.e.* the centres of the 6-rings of the framework. They are, however, systematically displaced in such a way that displacive modulation waves* result (Fig. 3). The phase relationships of these waves give rise to the characteristic intensity distribution of the superstructure reflections,* which was successfully exploited in the course of the structure determination. The main argument concerned the *z* components of Sr atoms. Chains of Sr atoms running along [001] are subject to longitudinal displacive modulation waves of wavelength |*c*|. It follows that Sr atoms, being *c*/2 apart, are in antiphase. Sr(1) and Sr(2) are at the nodes, Sr(3) at the antinode of the modulation waves. The 'starting values' for the various modulated Sr chains, with respect to given planes of constant *z*, is determined by the MoO_4 tetrahedra, being 'above' and 'underneath' each Sr atom on the (cubic) body diagonal. Sr(1) and Sr(2) are located between like MoO_4 tetrahedron edges, *viz.* between two H edges or two V edges, respectively, and no *z* shift results. On the other hand, Sr(3) is asymmetrically surrounded by one H and one V edge. It is found that Sr(3) atoms are

* Lists of observed and calculated Bragg intensities, Tables 2(*b*), 2(*c*), 2(*e*), 2(*f*), 3(*b*), 3(*c*), 3(*e*), 3(*f*) and Figs. 1(*a*)–1(*f*) have been deposited with the British Library Document Supply Centre as Supplementary Publication No. SUP 53579 (108 pp.). Copies may be obtained through The Technical Editor, International Union of Crystallography, 5 Abbey Square, Chester CH1 2HU, England.

* It should be noted that the modulation waves are rational or commensurate modulation waves. Correspondingly, the superstructure reflections are 'super' only with respect to the idealized cubic structure and they are ordinary reflections in $I4_1/acd$.

Table 3. *Important interatomic distances* (Å) *and angles* (°) *for* $Sr_8[Al_{12}O_{24}](MoO_4)_2$, *SAM*

E.s.d.'s are in parentheses and refer to the last digit given. Angled brackets, ⟨ ⟩, denote mean values or their e.s.d. (absolute). O_F and O_T denote framework and cage-anion O atoms, respectively.

(*a*) 293 K

Al(1)—O(11)	1·71 (3)	Al(2)—O(11)	1·75 (2)	Al(3)—O(13)	1·74 (3)
O(12)	1·73 (3)	O(14)	1·80 (3)	O(16)	1·72 (3)
O(13)	1·80 (2)	O(15)	1·67 (3)	O(13)′	1·74 (3)
O(16)	1·71 (2)	O(12)	1·72 (2)	O(16)′	1·72 (3)
O(11)—Al(1)—O(12)	123 (1)	O(11)—Al(2)—O(14)	103 (1)	O(13)—Al(3)—O(16)	118·8 (6)
O(13)	96 (1)	O(15)	107 (1)	O(13)′	103·6 (9)
O(16)	109 (2)	O(12)′	122 (1)	O(16)′	101·7 (8)
O(12)—Al(1)—O(13)	106 (1)	O(14)—Al(2)—O(15)	120 (2)	O(16)—Al(3)—O(13)′	104·3 (8)
O(16)	107 (2)	O(12)′	103 (1)	O(16)′	110·2 (8)
O(13)—Al(1)—O(16)	116 (1)	O(15)—Al(2)—O(12)′	103 (1)	O(13)—Al(3)—O(16)′	118·9 (6)
Al(4)—O(14)	4 × 1·75 (2)	Al(5)—O(15)	4 × 1·73 (2)	Al(1)—O(11)—Al(2)	137 (1)
O—Al(4)—O	2 × 122·2 (8)	O—Al(5)—O	2 × 121·5 (8)	Al(1)—O(12)—Al(2)′	158 (1)
	2 × 105·8 (9)		4 × 103·8 (8)	Al(1)—O(13)—Al(3)	136 (1)
	2 × 101·2 (9)			Al(2)—O(14)—Al(4)	147 (1)
				Al(2)—O(15)—Al(5)	150 (1)
				Al(1)—O(16)—Al(3)′	168 (1)
⟨Al—O⟩	1·7365⟨0·028⟩			O(1)—O(16)	3·10 (2)
⟨σ⟩	0·024			Mo—O(1)—O(16)	164 (1)
⟨O—Al—O⟩(wide)	120·6⟨2·05⟩			O(2)—O(12)	3·02 (2)
⟨O—Al—O⟩(narrow)	104·2⟨3·05⟩			Mo—O(2)—O(12)	166 (1)
⟨Al—O—Al⟩	149·3⟨11·2⟩				
Sr(1)—O(14)	2·60 (3)	Sr(2)—O(11)	2·63 (2)	Sr(3)—O(12)	2·53 (2)
O(14)′	2·60 (3)	O(11)′	2·63 (2)	O(13)	2·56 (3)
O(13)	2·67 (3)	O(14)	2·67 (3)	O(15)	2·57 (3)
O(13)′	2·67 (3)	O(14)′	2·67 (3)	O(11)	2·62 (2)
O(12)	2·79 (2)	O(16)	2·77 (3)	O(16)	2·66 (3)
O(12)′	2·79 (2)	O(16)′	2·77 (3)	O(15)′	2·79 (3)
O(2)	2·82 (2)	O(1)	2·85 (3)	O(1)	2·77 (3)
O(2)′	2·82 (2)	O(1)′	2·85 (3)	O(2)	2·88 (2)
⟨Sr(1)—O⟩	2·72⟨0·09⟩	⟨Sr(2)—O⟩	2·73⟨0·09⟩	⟨Sr(3)—O⟩	2·67⟨0·12⟩
⟨Sr—$O_{framework}$⟩	2·666⟨0·082⟩	⟨Sr—$O_{cage\ anion}$⟩	2·832⟨0·034⟩		
		Mo—O(1)	2 × 1·74 (2)		
		O(2)	2 × 1·78 (2)		

(*d*) 623 K

Al—O_F	1·733 (2)	Sr—O_F	2·664 (1)
O_F—Al—O'_F	2 × 120·1 (1)	Sr—O_T	2·877 (5)
	4 × 104·4 (1)		
Al—O_F—Al′	149·9 (1)	Mo—O_T	1·71 (1)

Table 4. *Temperature and composition-dependent quantities, with e.s.d.'s in parentheses*

Nominal temperatures are given. V_{ps} denotes the volume of the pseudocubic unit cell. The atomic displacement parameters U (× 10^3) were refined for sets of structurally equivalent atoms. The spontaneous strain was calculated using the relationship $\mu = \frac{1}{6}(e_{11} + e_{22} - 2e_{33})$, with $e_{11} = e_{22} = c/a$ and $e_{33} = 1$.

	SAM 293 K	SAM 423 K	SAM 523 K	SAM 623 K	SAM 723 K	SAW 293 K
Space group	$I4_1/acd$	$I4_1/acd$	$I4_1/acd$	$Im\bar{3}m$	$Im\bar{3}m$	$I4_1/acd$
a (Å)	18·8751 (6)	18·9057 (8)	18·9216 (8)	9·4643 (3)	9·4725 (3)	18·8770 (6)
c (Å)	18·7839 (9)	18·822 (1)	18·850 (1)	–	–	18·7816 (9)
V_{ps} (Å^3)	836·5 (1)	840·9 (1)	843·6 (1)	847·7 (1)	849·9 (1)	836·6 (1)
$V_{ps}^{1/3}$ (Å)	9·4223 (3)	9·4388 (3)	9·4488 (3)	–	–	9·4226 (3)
μ (× 10^4)	−16·8 (3)	−14·1 (3)	−12·6 (3)	–	–	−16·8 (3)
U(Al) (Å^2)	2 (1)	8 (1)	7 (1)	9 (1)	10 (1)	2 (1)
U(Sr) (Å^2)	13 (1)	20 (1)	20 (1)	32 (1)	38 (1)	12 (1)
$U(O_F)$ (Å^2)	5 (0)	14 (1)	14 (1)	22 (1)	24 (1)	5 (1)
U(Mo,W) (Å^2)	13 (1)	28 (3)	30 (1)	27 (4)	25 (4)	8 (3)
$U(O_T)$ (Å^2)	28 (1)	48 (3)	57 (3)	103 (6)	134 (8)	24 (1)

shifted towards the H edges. These z shifts may occur along the positive or negative z direction, depending on the actual arrangement of the Sr atom and associated H edge, and result in an antipolar, perhaps antiferroelectric, structure. The coordination sphere of each Sr atom consists of six oxygens of the surrounding crown-like 6-ring of the framework and of two oxygens belonging to two MoO_4 groups above and underneath the 6-ring. The coordination polyhedron thus formed is quite uncommon, as it is best described as a ditrigonal scalenohedron (Fig. 4). The Sr—O interatomic distances are normal with averages of 2·67 ⟨0·08⟩ and 2·83 ⟨0·03⟩ Å for Sr—O_F and Sr—O_T, respectively (O_F: framework oxygen;

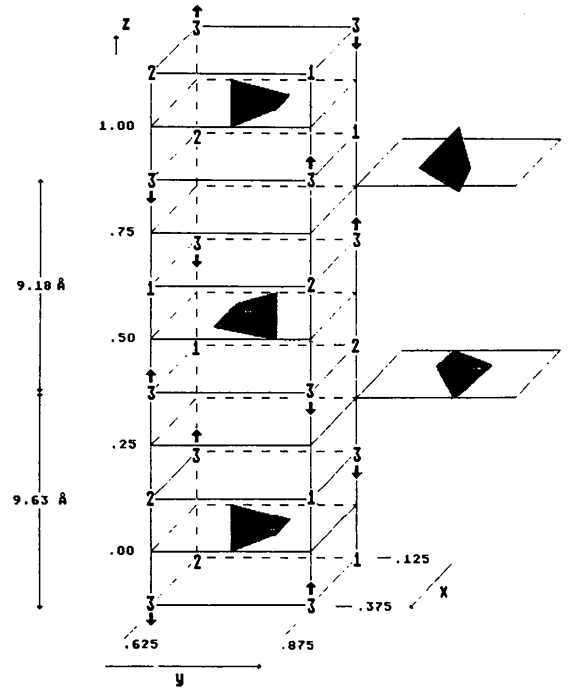

Fig. 2. Tetragonal phase of SAM. Only cage ions are shown. Numbers designate the Sr atoms. Cubes of Sr atoms surround MoO_4 tetrahedra, which are 'lying' with respect to the z direction. The Sr(1) and Sr(2) atoms are symmetrically coordinated by horizontal or vertical tetrahedron edges, respectively. For Sr(3) the coordination is asymmetric. The resulting z shift is indicated by an arrow. Distances between z-modulated Sr(3) atoms, given on the left-hand side, as well as the arrangement of arrows, indicate the antiphase relationship of the corresponding modulation waves. Some fractional coordinates are given along the x, y and z directions.

O_T: XO_4 tetrahedron oxygen). Here and in the following the values in angled brackets denote population standard deviations; the mean e.s.d. for the bonds is 0·03 Å. The asymmetrical coordination of Sr(3) again becomes noticeable in its uneven $Sr—O_T$ bond lengths.

The geometry of the framework constituents, *i.e.* the AlO_4 tetrahedra, conforms to the expected values (Depmeier, 1984*b*): mean *d*(Al—O) 1·74 ⟨0·03⟩ Å, mean e.s.d. 0·02 Å, mean wide angle O—Al—O (α) 121 ⟨2⟩°, mean narrow angle O—Al—O (α') 104 ⟨3⟩°. The mean angle Al—O—Al (γ) is 149 ⟨11⟩°. The important variance of this value results from the conformational shearing of the framework (*cf.* Depmeier, 1988*a*). The latter is characteristic of ordered aluminate sodalites, and is a consequence of the tetragonal orientation of the XO_4 groups and ensuing repulsive interactions between O_T and certain O_F atoms. In SAM this becomes noticeable in the significantly widened Al—O—Al angles at O(12) and O(16) (Table 3*a*). These atoms have short interatomic distances from the O_T atoms O(2) and O(1) of 3·02 (2) and 3·10 (2) Å, respectively. The widening of the angles at O(12) and O(16) is compensated by a corresponding narrowing of the angles at O(11) and O(13). O(11) and O(12), on one side, and O(13) and O(16), on the other side, form 4-rings of the framework, together with symmetrically equivalent atoms, which are heavily deformed by the shearing (Fig. 5). O(14) and O(15), both of which are unaffected by the just-mentioned 'positive' [O(12), O(16)] or 'negative' [O(11), O(13)] interaction, constitute an almost undeformed 4-ring (Fig. 5).

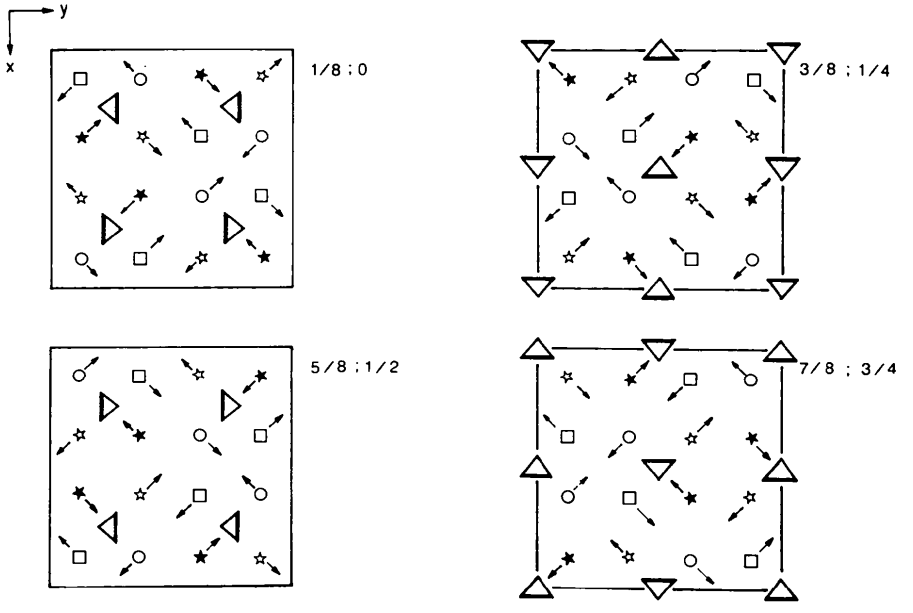

Fig. 3. The arrangement and modulation of cage ions in the tetragonal phase of SAM. Triangles indicate MoO_4 tetrahedra with the horizontal edge drawn as a thick line. The tetrahedra are at $z = 0 \bmod \frac{1}{4}$. Sr atoms are at $\frac{1}{8} \bmod \frac{1}{4}$. Circles, squares and stars represent Sr(1), Sr(2) and Sr(3) atoms, respectively. Deviations from the cubic positions are indicated by arrows in the *xy* plane, but by filled or empty symbols in the (+) or (−) z direction. Only Sr(3) atoms have significant z components in their modulation.

An analysis of its geometrical features demonstrates that the sodalite framework's deformation is almost completely explained by the conformational shearing. In particular, a contribution from a tilt mechanism is virtually negligible. In this sense the framework can be described as fully expanded. The shearing also accounts for the fact that the pseudocubic unit-cell volume is slightly reduced compared with an ideal zero-tilt zero-shear sodalite having a bond length equal to the mean d(Al—O) of SAM. Thus, the shearing contributes to the reduction of the unit-cell volume of sodalites, just as the tilt does. This explains also why an 'estimated tilt angle', different from 0°, could be calculated for SAM and SAW on the basis of the known unit-cell volumes (Depmeier, 1988*a*).

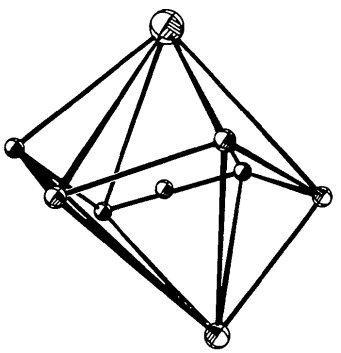

Fig. 4. The coordination of Sr [here Sr(2)] is well described by a ditrigonal scalenohedron. This is formed by the O atoms of a 6-ring of the sodalite framework (centre) and by two MoO_4 O atoms above and underneath the 6-ring.

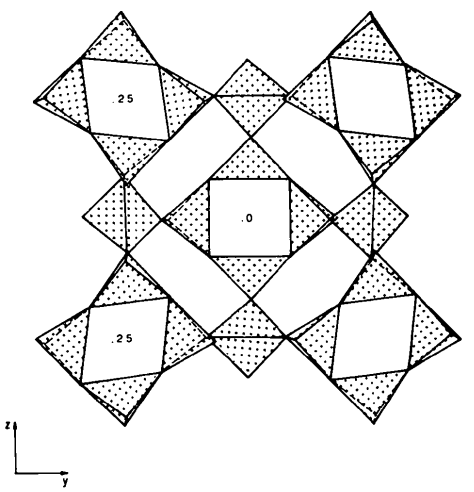

Fig. 5. Partial projection of the framework of tetragonal SAM along the x direction. At the corners one notices deformed 4-rings. This shearing is the result of repulsive interactions between framework O atoms (at the vertices of the tetrahedra) and MoO_4 groups (not shown). The 4-ring at the centre is not affected by such interactions and appears, therefore, normal.

The cubic phase

The cubic phase of SAM could be refined successfully in space group $Im\bar{3}m$. As in the cases of cubic CAW (Depmeier, 1988*b*) and SACr (Depmeier, Schmid, Setter & Werk, 1987), the cage anions are disordered over the various 'tetragonal orientations'. Similarly, interatomic distances and angles, uncorrected for thermal effects, correspond to the known cubic aluminate sodalites and structural parameters of the cubic phase match closely the corresponding average values of the ordered low-temperature phase. Some atomic displacement parameters are anomalous (see below).

Temperature-dependent studies

Although it was not the main purpose of the present work to study in detail the temperature dependence of SAM, we profitted by having some spare time at DMC and collected a few extra data sets. We set out to show that this rather crude experiment provides us with some useful information about the temperature dependence of SAM. Fig. 6 shows the lattice parameters for both phases of SAM, as well as the spontaneous strain and the cube root of the pseudocubic unit-cell volume for the tetragonal phase, as a function of temperature. The phase transition at $T = 571$ K is clearly visible. Tentatively, power laws have been fitted to the lattice parameters and spontaneous strain of tetragonal SAM, with critical exponents 0·15 and 0·12, respectively. Because of the small number of observations (three) and the uncertainty in the temperature measurement, these values should be regarded with due

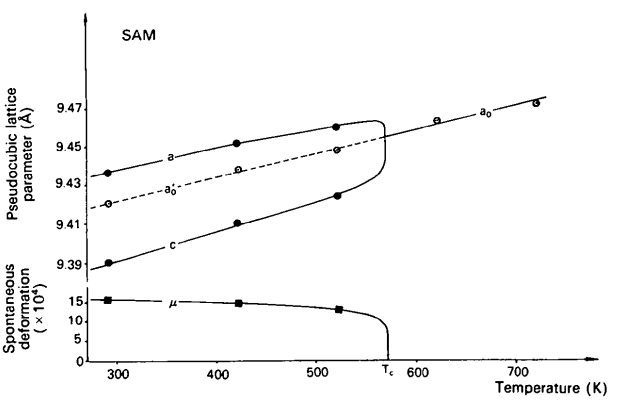

Fig. 6. Pseudocubic lattice parameters a, c, cubic lattice parameter a_0, and spontaneous strain μ as a function of temperature. $\mu = (e_{11} + e_{22} - 2e_{33})/6$, with $e_{11} = e_{22} = c/a$ and $e_{33} = 1$. a'_0 denotes the cube root of the pseudocubic cell volume. The straight line is a linear regression fit to a_0 and a'_0. Curved lines are power-law fits, obtained from log/log plots and using the data points indicated. Vertical error bars would be much smaller than, horizontal ones would be about, the size of the symbols used, neglecting a difference between real and set temperature of 30–40 K (see text).

caution and the corresponding curves considered as a mere guide for the eye. However, it is clear that the value found for the spontaneous strain does not correspond at all to what would be expected for pure mean-field behaviour with the spontaneous strain representing the primary order parameter of the phase transition. This is, of course, in accordance with the improper character of the phase transition, as shown by the formation of a superstructure below T_c. Future experiments have to collect more data, in particular in the critical region close to the phase transition, in order to get better fits.

To a first approximation the thermal expansion of $V^{1/3}$ is linear below T_c, and continues to be so in the cubic phase. The mean coefficient of approximately 12×10^{-6} K^{-1} compares well with values found for aluminosilicate sodalites (Henderson & Taylor, 1978). The resolution of our experiment does not allow a kink in the thermal-expansion curve at T_c to be confirmed or rejected with reasonable certainty. If a kink did not exist, then one would conclude, from the continuous character, that the mechanism of the thermal expansion is probably the same in both phases. Since the cubic phase is a zero-tilt phase, an 'unfolding' of the framework, as primary driving force for the thermal expansion of SAM, became improbable. Nor did the structure refinements with the various data sets reveal any other systematic trend among distances or angles, which would lend itself to a convincing explanation for the thermal expansion. At the present stage it therefore seems reasonable to assume that the thermal expansion in SAM is governed by the usual anharmonicity effects. However, the impossibility of detecting systematic trends may equally well be a consequence of the high estimated standard deviation of the structural parameters. It is clear that future experiments have to concentrate on the critical region close to T_c, where the most significant changes are to be expected. In addition, improved data-collection and evaluation techniques have to be employed (see *e.g.* Prince, 1984). Note that the values for interatomic distances and angles given here are not corrected for thermal effects.

Fig. 7 shows the atomic displacement parameters as a function of temperature. Regression lines have been fitted to the data of the low-temperature phase. The extension of the corresponding lines into the cubic phase fits the experimental values of the framework atoms Al and O_F quite well. The slope of the Al line ($\partial U/\partial T = 18 \times 10^{-6}$ Å^2 K^{-1}) agrees well with the corresponding value given by Hazen & Finger (1982), *viz.* 19×10^{-6} Å^2 K^{-1}. For the non-framework atoms the disagreement in the cubic phase is striking. In particular, the negative deviation of Mo from the regression line seems physically unrealistic. This and the opposite behaviour of the O_T atom suggest that this might be the result of a deficiency of the model used. It should be noted that the description of the disordered MoO_4 tetrahedron, with Mo and O_T on Wyckoff positions 2(*a*) and 24(*h*), respectively, is just the simplest crystallographic representation which fits into the standard refinement programs. Planned studies concentrating on the disorder in the cubic phases of aluminate sodalites surely will have to use more elaborate models. Abnormally high displacement parameters were also observed for cubic $Ca_8[Al_{12}O_{24}](WO_4)_2$, CAW, and could be explained by the assumption that the static translationally periodic distortions of the ordered phase become dynamic and non-periodic in the corresponding disordered phase (Depmeier, 1988*b*). The latter is cubic only on the space/time average. The argument required that the reorientational disorder of the cage anions is transferred as displacive disorder onto the framework atoms (rotation–translation coupling). Following this argument leads to the conclusion that the displacement parameters of the framework atoms Al and O_F of SAM correspond more closely to thermal vibration than in the case of CAW, where the corresponding, highly anomalous, displacement parameters express an important contribution from a 'wobbling' framework.

The average atomic positions of the ordered phases correspond, to a good approximation, to the cubic positions above T_c. Hence the idea that increased distortion of the ordered phase, *i.e.* shearing, leads to increased displacement parameters in the cubic phase. This idea finds support in the different values of the mean-square static deviation of Al

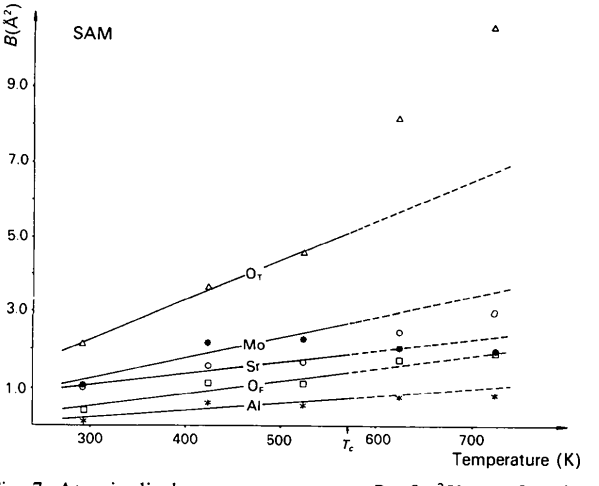

Fig. 7. Atomic displacement parameters $B = 8\pi^2 U$ as a function of temperature. Straight lines are linear-regression fits to data points below T_c. Above T_c only Al and O_F continue to follow the regression lines, whereas Sr, Mo and O_T deviate significantly. The latter behaviour is interpreted as indicating dynamical disorder.

from the average position in the corresponding ordered phase. This value is only 0·006 Å^2 for SAM, but 0·025 Å^2 for CAW. In this context it might be interesting to note that, at room temperature, the mean deviation from the cubic position is about 0·07 Å for Sr(1) and Sr(2), but 0·18 Å for Sr(3) (SAM). For the framework oxygens this value is about 0·18 Å, which may be compared with 0·30 Å for CAW.

The cubic–tetragonal phase transition of SAM; identification of the irreducible representation

We assume that the symmetry assignment is essentially correct, namely that the space groups of the cubic and the tetragonal phase are $Im\bar{3}m$ and $I4_1/acd$, respectively. The transition is associated with a change of the unit-cell size, *viz.* a doubling of all three conventional basic vectors. Fig. 8 shows the symmetry reduction in terms of group–maximal subgroup relations. From this the (augmented) matrix for the transformation from cubic to tetragonal atomic coordinates could be deduced. Row by row it reads ($\frac{1}{2}$,0,0,0; 0,$\frac{1}{2}$,0,0; 0,0,$\frac{1}{2}$,$-\frac{1}{4}$; 0,0,0,1). For $I4_1/acd$ origin choice 2 was chosen, which puts the origin at an inversion centre (*International Tables for Crystallography*, 1987, Vol. A). With respect to the structure the origin moves at the transition from the centre of a sodalite cage to the centre of a 4-ring, just half a cubic lattice constant above the old origin. In the tetragonal phase the centres of the cages are no longer centrosymmetric. As these are the loci of the cage anions, ordered XO_4 tetrahedra are permitted.

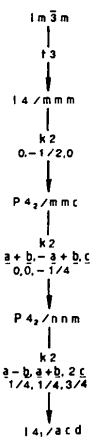

Fig. 8. The proposed symmetry reduction *via* smallest steps of maximal subgroups from the high-temperature phase of SAM(SAW) with space group $Im\bar{3}m$ to the room-temperature phase with space group $I4_1/acd$ (origin choice 2). The index of the group–subgroup relationship is given as well as its type, *viz.* *t* for *translationengleich* and *k* for *klassengleich*. Unit-cell transformations and shifts of the origin are also indicated.

The lowest-rank macroscopic tensor property that distinguishes the two phases is the strain tensor. The transition may therefore be classified as ferroelastic. The spontaneous strain, however, cannot represent the primary order parameter, because the transition is improper, as proved by the formation of a superstructure. This fact also becomes noticeable in the temperature dependence of the spontaneous strain (see above).

Mathematical group–subgroup relations are useful for various reasons. They fail, however, to predict which subgroup may become physically realized in the event of a phase transition. A more appropriate approach is to relate possible physical distortions to symmetry *via* space-group representations. This is the realm of Landau and related theories. Stokes & Hatch (1988) have tabulated the 'isotropy subgroups' of the 230 space groups, together with useful additional information. In their tables we find, for $Im\bar{3}m$ as parent symmetry, four irreducible representations leading to $I4_1/acd$ as subgroup. They are labelled N_3^+, N_4^+, N_1^- and N_2^-. The first two possibilities can be excluded, as they require a shift of the origin, such that the inversion centre would coincide with the centre of a sodalite cage. This is incompatible with ordered XO_4 tetrahedra.

The N_1^-, as well as the N_2^-, irreducible representation correctly places the inversion centre on the 4-ring and requires a doubling of all three conventional basic vectors. Thus, either N_1^- or N_2^- can be regarded as the active representation driving the cubic–tetragonal phase transition of SAM (and SAW). The tables of Stokes & Hatch (1988) also allow the derivation of the direction of the six-component order parameter and construction of the Landau potential. Their discussion is beyond the scope of this paper. The tables indicate, furthermore, that the phase transition is allowed to be continuous in Landau theory (but not in renormalization group theory). Of course, this does not mean that the transition must be continuous. Much more precise work than in the present study is required to establish the continuous or discontinuous character of the structural changes which represent the primary order parameter of the phase transition.

Tetragonal SAM (SAW) as a (3 + 3)-dimensionally modulated structure

In contrast to incommensurate crystal phases, commensurately modulated crystals can be described adequately using a three-dimensional space group. Occasionally, however, it may become more convenient to employ the superspace-group approach (de Wolff, Janssen & Janner, 1981). Such may be the case if the modulated character of a crystal structure should be emphasized, or if one has to limit the

number of variables in a structure refinement. The following is based on Janner, Janssen & de Wolff (1983*a*,*b*). The diffraction pattern of tetragonal SAM, or SAW, can be divided unambiguously into sets of main reflections and of satellite reflections. Main reflections are those which become the cubic reflections above T_c. They correspond to a (pseudo-cubic) tetragonal I lattice. The main reflections are surrounded cuboctahedrally by satellite reflections $(h+\alpha,\ k,\ l+\theta)$, $(h,\ k+\alpha,\ l+\theta)$, $(h+\alpha,\ k+\alpha,\ l)$. These can be described by linear combinations of basic modulation vectors $q_1=(\alpha,0,0)$, $q_2=(0,\alpha,0)$ and $q_3=(0,0,\theta)$. For the sake of simplicity it is assumed that α and θ deviate slightly from the rational value $\frac{1}{2}$. The positions and intensities of all reflections with wavevectors $k=ha^*+kb^*+lc^*+m_1q_1+m_2q_2+m_3q_3$ are invariant under the point group of the pattern of main reflections. Hence the Bravais class is $I4/mmm$ $(\alpha,0,0;\ 0,0,\theta)$, *i.e.* No. 3-170 in Table 1 of Janner, Janssen & de Wolff (1983*a*). A preliminary attempt to apply the superspace approach was undertaken by Yamamoto (1988). He used the X-ray single-crystal data of SAM 11/82, which have been reported earlier as including a considerable number of questionable reflections (see *Experimental*). The refinement, employing the *REMOS*82 (Yamamoto, 1982) program, did not converge. Without a proof to the contrary it is assumed that this failure is attributable to the low crystal quality.

We are grateful to M. Ruedlinger for his contribution to the computational analysis of the data.

References

DEPMEIER, W. (1984*a*). *Acta Cryst.* C**40**, 226–231.
DEPMEIER, W. (1984*b*). *Acta Cryst.* B**40**, 185–191.
DEPMEIER, W. (1988*a*). *Phys. Chem. Miner.* **15**, 419–426.
DEPMEIER, W. (1988*b*). *Acta Cryst.* B**44**, 201–207.
DEPMEIER, W., SCHMID, H., SETTER, N. & WERK, M. L. (1987). *Acta Cryst.* C**43**, 2251–2255.
FISCHER, P. (1985). *IUCr Neutron Diffr. Newsl.* (April 1985), pp. 15–16.
FLACK, H. D. (1987). *Acta Cryst.* A**43**, 564–568.
HAZEN, R. M. & FINGER, L. W. (1982). *Comparative Crystal Chemistry*. New York: John Wiley.
HENDERSON, C. M. B. & TAYLOR, D. (1978). *Phys. Chem. Miner.* **2**, 337–347.
JANNER, A., JANSSEN, T. & WOLFF, P. M. DE, (1983*a*). *Acta Cryst.* A**39**, 658–666.
JANNER, A., JANSSEN, T. & WOLFF, P. M. DE, (1983*b*). *Acta Cryst.* A**39**, 671–678.
PRINCE, E. (1984). *Acta Cryst.* A**40** (Suppl.), C-433.
RIETVELD, H. M. (1969). *J. Appl. Cryst.* **2**, 65–71.
SETTER, N. & DEPMEIER, W. (1984). *Ferroelectrics*, **56**, 45–48.
SETTER, N., MENDOZA-ALVAREZ, M.-E., DEPMEIER, W. & SCHMID, H. (1984). *Ferroelectrics*, **56**, 49–52.
STOKES, H. T. & HATCH, D. M. (1988). *Isotropy Subgroups of the 230 Crystallographic Space Groups*. Singapore: World Scientific.
WILES, D. B. & YOUNG, R. A. (1981). *J. Appl. Cryst.* **14**, 149–151.
WOLFF, P. M. DE, JANSSEN, T. & JANNER, A. (1981). *Acta Cryst.* A**37**, 625–636.
YAMAMOTO, A. (1982). *REMOS*82. A computer program for the refinement of modulated structures. National Institute for Research in Inorganic Materials, Tsukuba, Ibaraki 305, Japan.
YAMAMOTO, A. (1988). Private communication.

Acta Cryst. (1991). B**47**, 206–209

Structure of Oxonium Hexafluoroantimonate(V)

BY E. M. LARSON*

Chemistry and Materials Science Department, Lawrence Livermore National Laboratory, Livermore, CA 94550, *USA*

AND KENT D. ABNEY,† ALLEN C. LARSON‡ AND P. GARY ELLER†

Los Alamos National Laboratory, Los Alamos, NM 87545, *USA*

(*Received* 30 *April* 1990; *accepted* 22 *October* 1990)

Abstract. $[H_3O][SbF_6]$, $M_r=2038{\cdot}09$, cubic, $I2_13$, $a=10{\cdot}120\ (7)$ Å, $V=1036{\cdot}43$ Å^3, $Z=8$, $D_x=3{\cdot}265$ g cm^{-3}, $\lambda(\text{Mo } K\alpha_1)=0{\cdot}70930$ Å, $\mu=54{\cdot}09$ cm^{-1}, $F(000)=928$, $T=238$ K, $R=0{\cdot}059$ and $wR=0{\cdot}045$ for 288 reflections with $F_o\geq 3\sigma(F_o)$. Antimony lies at the center of a somewhat distorted octahedral array [F—Sb—F = 84·4 (3), 87·3 (3), 92·2 (4), 95·6 (4) and 171·3 (4)°, with Sb—F = 1·891 (7) and 1·854 (9) Å] of F atoms. Three fluorines are connected to the O atoms through hydrogen bonds as indicated by the F—O distances of 2·622 (12) Å and the other three F atoms have

* Address correspondence to this author.
† Isotope and Nuclear Chemistry Division.
‡ Manuel Lujan Jr Neutron Scattering Center, LANSCE.

0108-7681/91/020206-04$03.00